47.4: Blue Phosphorescent Organic Light Emitting Device Stability Analysis

Brian W. D'Andrade, Michael S. Weaver, Peter B. Mackenzie, Hitoshi Yamamoto, and Julie J. Brown
Universal Display Corp., Ewing, NJ 08618

Noel C. Giebink, Stephen R. Forrest
Department of Electrical Engineering and Computer Science and Physics, University of Michigan, Ann Arbor, MI 48109

Mark E. Thompson
Department of Chemical Engineering and Materials Science, and Department of Chemistry, University of Southern California, Los Angeles, CA 90089

Abstract
A model based on defect generation by exciton-polaron annihilation interactions between the emitter and host molecules, in a blue phosphorescent OLED, is shown to fit well with experimental data. A blue PHOLED with (0.15, 0.25) chromaticity is shown to have a half-life, from 1,000 nits, of 690 hrs.

1. Introduction
The operational stability of blue phosphorescent organic light emitting devices (PHOLED™s) [1] presents a challenge to their wide-spread acceptance for use in large-area displays and solid-state lighting [2]. However, the steady progress in green and red PHOLED efficiencies and lifetime are testament to the strengths of phosphorescent emitters to provide long operational lifetime with high efficiency. Table I shows the state of the art for PHOLED device performance. Green and red PHOLEDs have high efficacies and long lifetime to meet the specifications for display applications, and these characteristics have been engineered through the development of synthetic and fabrication processes, materials design and device architectures.

A deep understanding of device failure is still needed to achieve similar performance characteristics for saturated blue PHOLEDs. The *intrinsic* luminance loss and voltage rise accompanying long term device operation are not well understood [3], and various hypotheses have been offered to explain the basis for intrinsic degradation in device efficiency, with the most widely accepted advocating chemical degradation of a fraction of the emissive molecules [2].

Presumably, bond cleavage produces radical fragments, which then participate in further radical addition reactions to form more degradation products. These products act as non-radiative recombination centers, luminescence quenchers, and deep charge traps. For example, evidence has recently been presented that the excited states themselves may form reaction centers in the case of the common host material 4,4'-bis(9-carbazolyl)-2,2'-biphenyl (CBP) [4].

Table I. PHOLED performances are listed. The data are based on various device structures and support materials processed using vacuum thermal evaporation. The operational lifetime data are based on accelerated current drive conditions at room temperature.

PHOLEDs	CIE COLOR COORDINATES	EXTERNAL QUANTUM EFFICIENCY (%)	LUMINOUS EFFICIENCY (cd/A)	OPERATIONAL LIFETIME TO 50% L. (HRS)	INITIAL LUMINANCE (cd/m²)
DEEP RED	(0.68, 0.32)	15	11	80,000	1,000
	(0.67, 0.33)	18	19	90,000	1,000
	(0.66, 0.34)	22	27	200,000	1,000
RED	(0.65, 0.35)	20	24	300,000	1,000
	(0.64, 0.36)	20	28	330,000	1,000
YELLOW-GREEN	(0.44, 0.55)	18	62	180,000	1,000
GREEN	(0.36, 0.61)	15	56	75,000	1,000
	(0.38, 0.59)	19	67	250,000	1,000
	(0.33, 0.63)	10	37	40,000	1,000
LIGHT BLUE	(0.16, 0.29)	11	21	3,000	500
	(0.16, 0.27)	8	14	9,000	500
BLUE	(0.14, 0.13)	4	9	UNDER DEVELOPMENT	500
WARM WHITE	(0.47, 0.45)	14	28	21,000	1,000
WHITE	(0.38, 0.39)	20	33	4,000	1,000

 ISSN/008-0966X/08/3902-0712-$1.00

Here, we study the degradation characteristics of a blue phosphorescent OLED (PHOLED) using 3,3'-di(9*H*-carbazol-9-yl)biphenyl (mCBP) as the host. A model is developed that describes device luminescence degradation, voltage rise, and emissive layer photoluminescence quenching of electrically aged devices. We find that defect generation due to exciton-polaron annihilation is consistent with the observed degradation effects.

2. Model

Defects can act as luminescent quenchers, non-radiative recombination centers, and deep charge traps. Luminance loss results from the first two, while voltage rise, which has been linked to the presence of fixed space charge in the emissive region can result from filling of the deep traps.

Defects are assumed to act only as hole traps. In addition, the defect state itself may not lead directly to a quenching transition, but when occupied with a trapped charge, the resulting polaron may become a quenching center.

We assumed a single recombination zone that decays exponentially from one edge of the emissive layer (EML) with characteristic length d_{rec}. Excitons either form directly on guest molecules, or they are rapidly transferred from the host due to the high doping concentration and the possibility for exothermic energy transfer. Due to the high host triplet energy, guest excitons are strongly localized, leading to a negligible possibility for diffusion out of the recombination zone.

These considerations lead to rate equations for hole (p), electron (n), and exciton (N) densities in the recombination zone as follows:

$$\frac{dp(x,t,t')}{dt} = \frac{J}{qd_{rec}\left(1-\exp\left(\frac{-(x_2-x_1)}{d_{rec}}\right)\right)}\exp\left(\frac{-(x-x_1)}{d_{rec}}\right) - \gamma n(x,t,t') - \sigma \upsilon_{th}[f_D(E_t)]Q(x,t')p(x,t,t') \quad [1]$$

$$\frac{dn(x,t,t')}{dt} = \frac{J}{qd_{rec}\left(1-\exp\left(\frac{-(x_2-x_1)}{d_{rec}}\right)\right)}\exp\left(\frac{-(x-x_1)}{d_{rec}}\right) - \gamma n(x,t,t') - \gamma_2[1-f_D(E_t)]Q(x,t')n(x,t,t') \quad [2]$$

$$\frac{dN(x,t,t')}{dt} = \gamma n(x,t,t')\,p(x,t,t') - \left(\frac{1}{\tau} + K_{DR}Q(x,t')\right)N(x,t,t') \quad [3]$$

The electron, hole, and exciton densities depend on the time scale of transport and energy level transitions, t (short), as well as on that of degradation, t' (long), due to formation of defects of density $Q(x,t')$. The electron and hole densities are functions of the current density, J, the elementary charge q, and the device dimensions shown in Fig. 1. Excitons are formed at the Langevin rate $\gamma = q(\mu_n + \mu_p)/\varepsilon\varepsilon_0$ and decay with natural lifetime, τ. The hole and electron mobilities in the doped emissive layer are $\mu_n = 8\text{x}10^{-8}$ $\text{cm}^2\text{V}^{-1}\text{s}^{-1}$ and $\mu_p = 2\text{x}10^{-7}$ $\text{cm}^2\text{V}^{-1}\text{s}^{-1}$ respectively, the relative dielectric constant of the emissive layer is $\varepsilon \approx 3$, and ε_0 is the permittivity of free space.

In Eq. (1), holes with thermal velocity, $\nu_{th}\sim 10^7$cm/s, trap at defect sites of energy, E_t, and cross section, σ. The Fermi factor, $f_D(E_t) = [\exp(E_t - E_{Fv}) + 1]^{-1}$, gives the probability that the hole trap is empty, where E_{fv} is the hole quasi-Fermi energy. Electrons in Eq. (2) non-radiatively recombine at a rate proportional to the trapped hole density, $Q(x,t')[1-f_D(E_t)]$, and the reduced Langevin coefficient, $\gamma = q(\mu_n)/\varepsilon\varepsilon_0$, since trapped holes are assumed to be immobile. Quenching of excitons by defects is described by the bimolecular rate coefficient, K_{DR}, in Eq. (3). Note that only the constant prefactors change if defects trap electrons, or both carrier types, instead of only holes, as considered above.

One possible mechanism for defect generation mechanism is exciton-polaron annihilation, which can be described by Eq. (4).

$$\frac{dQ(x,t')}{dt'} = K_x N(x,t'), \quad K_x N(x,t')p(x,t') \quad [4]$$

Here, the rate constant, K_X, is consistent in dimension with the order of the reaction, exciton-polaron (hole or electron) annihilation in Eq. 4 is responsible for defect formation.

On the long time scale, t', Eqs. (1)-(3) are at steady state and can be solved to yield an expression for $N(x,t')$. The resulting, coupled differential equations containing $N(x,t')$ and $Q(x,t')$ are then solved numerically. Thus, the normalized OLED luminescence as a function of time is:

$$EL_{norm}(t') = \int_{x1}^{x2} N(x,t') \Big/ \int_{x1}^{x2} N(x,0) \quad [5]$$

Here, the integration limits, x_1 and x_2, are defined in Fig. 1 inset. The density of trapped charge increases with defect density following $\rho_T(x,t') = qQ(x,t')[1-f_D(E_t)]$. Assuming that the growth of ρ_T is offset by an equal density of opposing charge at the cathode, and that the free charge distributions under steady-state operation are not perturbed, then the voltage rise is given by:

$$\Delta V(t') \approx \int_0^{x3} x\rho_T(x,t')dx \quad [6]$$

The emissive layer photoluminescence (PL) transient will also be affected by defects. From Eq. (3) at time, t', the PL intensity normalized to that at $t = 0$ is:

$$PL_{norm}(t) = \frac{\int_{x1}^{x2} I_0(x)\exp\left[-\left(1/\tau + K_{DR}Q(x,t')\right)t\right]}{\int_{x1}^{x2} I_0(x)} \quad [7]$$

Here, $I_0(x)$ is the intensity profile of the excitation pulse in the device emissive layer calculated by the transfer matrix method for the specific device structure, incident excitation angle, wavelength, and polarization considered.

3. Experimental

Indium-tin-oxide (ITO) coated glass was cleaned with solvents and patterned into 2 mm^2 anode contact areas using standard photolithography techniques prior to organic film deposition. The ITO was oxygen plasma cleaned, exposed to UV-ozone treatment, and then loaded into a vacuum chamber with a base pressure of 10^{-7} Torr. The device structure is as follows (see Fig. 1, inset): a 10nm thick hole injection layer, a 30nm thick layer of the hole transporting, 4'-bis[N-(1-naphthyl)-N-phenyl-amino]-biphenyl (NPD), a 30 nm thick emissive layer consisting of mCBP doped with 9wt% of a blue phosphor and a 5 nm thick layer of mCBP for exciton confinement within the EML. Electrons are injected into the EML through a 40 nm thick layer of tris-(8-hydroxyquinoline) aluminum, capped by a cathode consisting of 0.8 nm thick layer of LiF and a 100 nm thick Al film. Following deposition, the PHOLEDs were transferred directly from vacuum into an oxygen and moisture-free N_2 glove box, where they were encapsulated using a UV-curable epoxy, and a glass lid containing a moisture getter.

External quantum efficiency (EQE) and power efficacy were

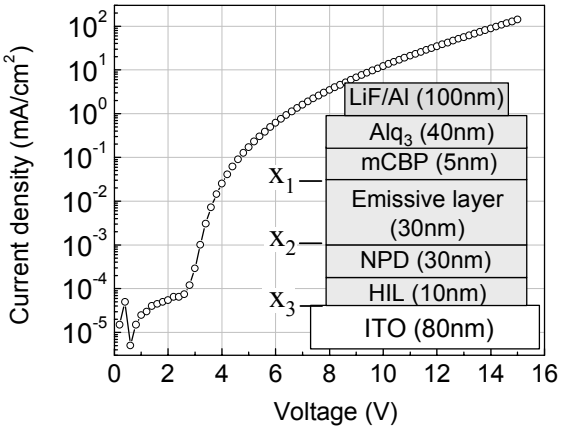

Figure 1. Typical J-V characteristics of the devices studied. Inset: schematic of the device structure, with the positions, x_1-x_3.

calculated from the spectral intensity measured normal to the substrate using a SpectraScan PR705. The current versus voltage measurements were obtained using a Keithley 236 source measurement unit. Operational lifetime measurements were performed at room temperature, and devices were aged at various constant currents while monitoring their operational voltage and light output. Photoluminescence transients were obtained periodically during electrical aging using a time-correlated single photon counting system from Horiba Jobin Yvon, with a 335 nm wavelength excitation source incident at 45º from normal, and emission was obtained at λ = 470 nm.

4. Results and Discussion

The current density-voltage (J-V) characteristics and EQE for the PHOLEDs taken immediately following fabrication are plotted in Figs. 1 and 2, respectively. The device shows a peak forward viewing EQE of 11%. The electroluminescence spectrum at J=10 mA/cm^2, with a peak at 464 nm and CIE (0.15, 0.25), is due to the dopant and remains the same at all current densities, indicating that the recombination zone remains within the EML.

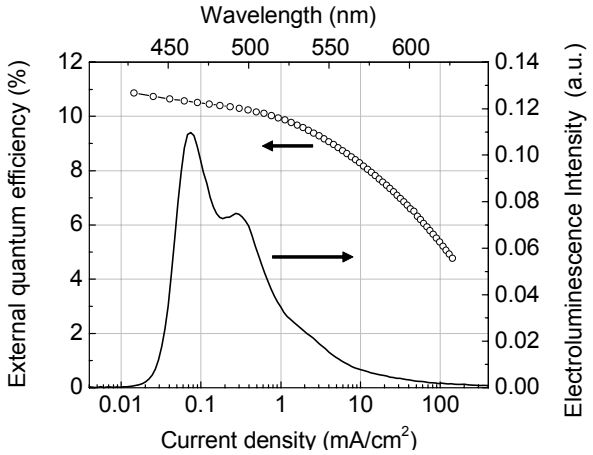

Figure 2. External quantum efficiency (left scale) and emission spectrum (right scale) obtained at J =10 mA/cm^2.

Figure 3 provides the normalized luminance versus time for four different drive current densities: 6.9, 15.1, 24.3 and 34.4 mA/cm^2 corresponding to initial (t' = 0) luminances of L_0 = 1000, 2000, 3000, and 4000 cd/m^2, respectively. The operational lifetime, LT_{80}, corresponds to the time required for the luminance to degrade to $0.8L_o$. The rate of luminance loss increases monotonically with J; here lifetimes decrease from 110 hrs at 6.9 mA/cm^2, to 9 hrs at 34.4 mA/cm^2. The solid lines in Fig. 3 are derived from the model. The voltage rise corresponding to the luminance loss is plotted in Fig 4.

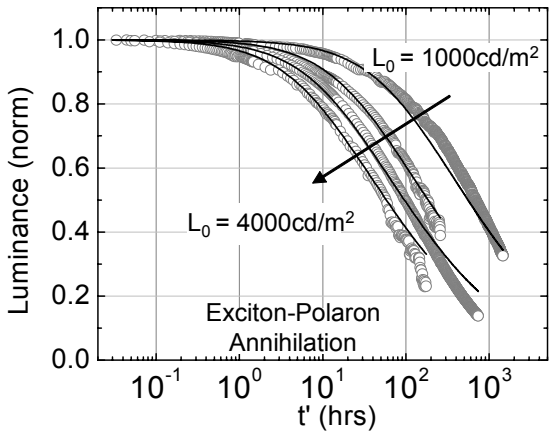

Figure 3. Luminance versus time experimental data are overlaid with solid black lines fits.

Figure 5 show PL transients obtained from an as-grown device, a device degraded to a luminance at time t' of $L(t')$=0.59, and one degraded to $L(t')$ = 0.16. The fit to the model is shown by solid lines.

The as-grown device shows a natural decay lifetime of 1.1 μs, while the degraded device transients become increasingly nonlinear, indicative of the existence of quenching. Fluorescence from NPD at 470 nm is responsible for the sharp decrease in intensity near t = 0. The transients are, therefore, normalized at the onset of phosphorescence, after the fluorescence has decayed to a negligible level (i.e. at t > 0.2μs).

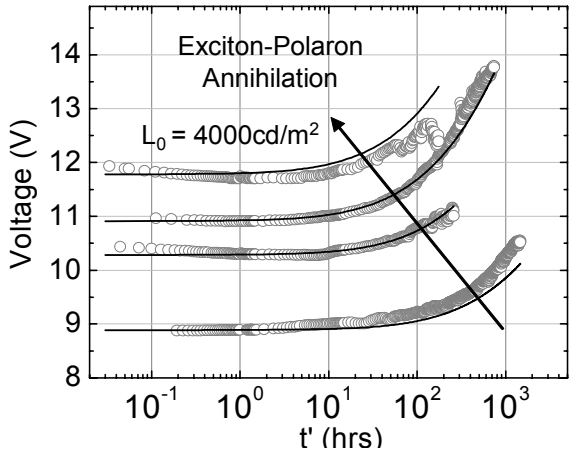

Figure 4. Voltage change with time corresponding to device data in Fig. 3. Solid lines are fits.

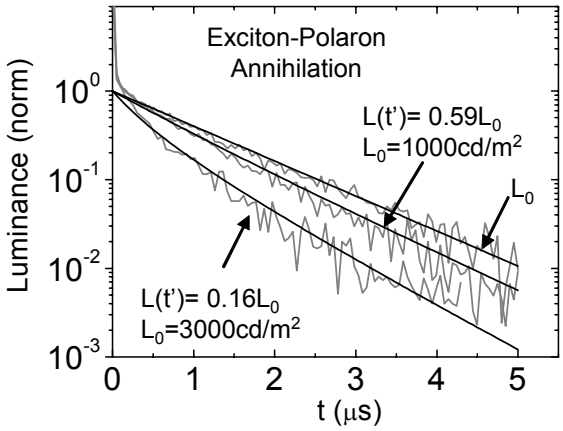

Figure 5. Photoluminescence transients obtained for an as-grown device, one aged to *L(t')* = 0.59 and 0.16 of the initial luminance, L_o. Solid black lines are fits

The exciton-polaron annihilation model results in a good fit across the entire range of data. In Fig. 3, the model deviates slightly in advanced stages of degradation ($L(t')<0.4L_o$), where the data show lower luminance than predicted. This may result from a change in charge balance due to the voltage rise (see Fig. 4), which results in higher polaron densities, and thus to an increased rate of degradation, providing a positive feedback not considered in the model.

The parameters d_{rec} = (8±2) nm, K_{DR} = (5±3)x10^{-12} cm^{3}s^{-1}, K_x = (7±2)x10^{-24} cm^{3}s^{-1} are consistent with expectations for this guest-host materials combination. For example, the values suggest that defect hole traps are nearly full, lying at ~0.1 eV above the hole quasi-Fermi level. Characteristic recombination lengths are all consistent with literature reported values of between 8 nm and 12 nm. Also, the defect exciton quenching rate, K_{DR}, is similar to that reported for other bimolecular quenching reactions in OLEDs [5]. Low capture cross-sections of σ~10^{-17} cm^{-3} result from localization of large effective mass holes that are characteristic of organic molecules.

Guest triplet excitons and host polarons are likely to be the dominant participants in the exciton-polaron defect formation reactions. The guest exciton density is much higher than the density on the host, since lifetimes on the host are short (<1ns) due to rapid energy transfer to the guests, where they exist as triplets for ~1μs. Since both Förster and exchange exciton-polaron annihilation mechanisms are strongly distance dependent, the physical separation of guests discourages guest-guest annihilations. We therefore infer that energy exchanged by annihilation of the guest triplet exciton to the host polaron results in a dissociative process of the host molecule itself. The fragments are in close proximity to the guest molecule and thus quench any subsequent triplets on that molecule, rendering it a permanent non-radiative center. Furthermore, as noted above, the fragmented molecule also acts as a deep trapping center, resulting in the observed operating voltage rise.

5 Summary

We find that defect generation due to exciton-polaron annihilation interactions in blue PHOLEDs between the dopant and host molecules leads to model predictions in good agreement with experimental lifetime data.

6. References

[1] M. S. Weaver, R. C. Kwong, V. A. Adamovich, M. Hack and J. J. Brown. "Latest developments in phosphorescent OLEDs." Proc. of International Meeting on Information Display, Vol. **2**, pp 1129-1132, 2006.

[2] H. Aziz and Z. D. Popovic, "Degradation phenomena in small-molecule organic light-emitting devices." Chem. Mat., Vol. **16**, pp 4522-4532, 2004.

[3] D. Y. Kondakov, J. R. Sandifer, C. W. Tang, and R. H. Young, "Nonradiative recombination centers and electrical aging of organic light-emitting diodes: Direct connection between accumulation of trapped charge and luminance loss." J. Appl. Phys., Vol. **93**, pp. 1108-1119, 2003.

[4] D. Y. Kondakov, W. C. Lenhart, and W. F. Nichols, "Operational degradation of organic light-emitting diodes: Mechanism and identification of chemical products." J. Appl. Phys., Vol. **101**, pp. 024512, 2007.

[5] S. Reineke, K. Walzer, and K. Leo, "Triplet-exciton quenching in organic phosphorescent light-emitting diodes with Ir-based emitter." Phys. Rev. B, Vol. **75**, pp. 125328-1 125328-13, 2007.